On Relay Selection for Relay-Assisted D2D Communications with Adaptive Modulation and Coding in Cellular Systems

Xixi Bi[1], Ruofei Ma[1,2](✉), Zhiliang Qin[2], and Gongliang Liu[1]

[1] Harbin Institute of Technology, Weihai 264209, Shandong, China
19S130290@stu.hit.edu.cn, {maruofei,liugl}@hit.edu.cn
[2] Beiyang Electric Group Co. Ltd., Weihai, Shandong, China
qinzhiliang@beiyang.com

Abstract. Developing device-to-device (D2D) communications can improve spectrum efficiency and traffic offloading capability of cellular systems. But only considering direct D2D communication mode may limit these benefits brought in by D2D communications, for direct D2D mode may not be available due to the long separation distance and poor link quality. Hence, relay-assisted D2D communication is presented to expand the coverage of D2D communications. One of the key points in developing relay-assisted D2D communication is to find out the optimal relay user equipment (UE) to assist data transmission between the source and destination D2D-capable UEs. In this paper, a cross-layer relay selection scheme is researched, which considers the end-to-end data rate, end-to-end transmission delay, and remaining battery time of the relay-capable UEs. Specially, we propose a method to estimate the end-to-end transmission delay for the relay-involved D2D path when adaptive modulation and coding (AMC) is taken into account. Performances of the proposed scheme are also evaluated.

Keywords: Device-to-device (D2D) communication · Relay selection · Transmission delay · Adaptive modulation and coding

1 Introduction

With increasing of wireless applications, it is important to develop new technologies to improve the spectrum efficiency. Amongst these technologies, device-to-device (D2D) communication is considered as one of the most promising way. D2D communication enables reducing the burden of cellular network by

This work was supported partially by National Natural Science Foundation of China (Grant No. 61801144, 61971156), Shandong Provincial Natural Science Foundation, China (Grant No. ZR2019QF003, ZR2019MF035), and the Fundamental Research Funds for the Central Universities, China (Grant No. HIT.NSRIF.2019081).

X. Wang et al. (Eds.): 6GN 2020, LNICST 337, pp. 127–143, 2020.
https://doi.org/10.1007/978-3-030-63941-9_10

allowing two proximity user equipments (UEs) to communicate directly bypassing the base station (BS) [1]. In addition, D2D communications can improve the performances on energy efficiency and system-wise throughput [2]. Hence, corresponding topics of D2D communications have attracted many scholars to research and investigate. According to whether or not using relay node during data transmissions, D2D communications can be commonly divided into direct and relay-assisted D2D communications. At present, most works of D2D communications focus on direct D2D communications, which commonly considers two types of D2D modes. One is dedicated D2D mode and the other is reuse D2D mode. Direct D2D pair in dedicated mode requires dedicated cellular radio resources [3], whereas the one in reuse mode needs to reuse the channel that is being used by a general cellular UEs (CUE), i.e., a CUE shares the same cellular spectrum resources with the D2D pair. Involving reuse mode can improve spectrum efficiency, while it also causes interference between D2D UEs and CUEs. Thus, there are many works concentrating on how to choose reuse channels and how to assign powers for D2D UEs and CUEs to limit the interference in the reuse mode [4–7]. However, it might not be enough while only considering direct D2D communications, because direct D2D communication probably can not be performed due to long separation distance between the source and destination D2D-capable UEs (DUEs) [8]. Hence, to expand the communication range of D2D communications and further enhance the system capacity and spectrum efficiency, including relay-assisted D2D mode may be a promising way [9,10].

A crucial problem on developing relay-assisted D2D communications is to find out the optimal relay-capable UE (RUE) for the DUEs in relay-assisted D2D mode under the BS scheduling. Thus, many criterias of choosing relay for relay-assisted D2D communications have been proposed, e.g., throughput, data rate, link outage probability, and power consumption, which are all designed on physical layer (PHY) [11,12]. To get an overall good performance via selecting the optimal relay, high layer criteria and remaining battery of the candidate RUEs need also to be considered. In [13], the transmission delay combining the packet buffer of relay is proposed, whereas, ignoring the packet buffer of the source UEs. In [14], authors proposes a cross-layer relay selection scheme combining the queue state information (QSI) of buffer for relay UEs, also ignoring the buffer of the source.

Base on the above analysis, cross-layer scheme should be considered more for its better overall performance. However, on the aspect of the delay estimate, most works only concentrate on the buffer of the relay, and lack comprehensive end-to-end cross-layer design. Also, the battery of the relay should also be considered as it has influences on the operation time of relay-assisted D2D communications, thus we proposed a cross-layer relay selection scheme which combines the end-to-end data rate, end-to-end delay and RUE remaining battery time in our previous work [15]. But the previous research we did ignores the time-varying of channels. To overcome this shortage, in this paper, on the aspect of the end-to-end delay, we investigate a new scheme combining the end-to-end delay with adaptive modulation and coding (AMC). Accordingly, in this paper, we only talk about derivation of the end-to-end delay with AMC, and the derivation of the end-to-end data rate and RUE remaining battery time can be found in the aforementioned work [15]. But on the performance evaluation, we will jointly assess the performance of the three criterias.

The rest of the paper is organized as follows. In Sect. 2, a single-cell system model for D2D communications is described. Section 3 introduces the problem formulation for relay selection. AMC technology is briefly introduced in Sect. 4. Section 5 provides the derivation process of end-to-end transmission delay for the relay-assisted D2D path, while Sect. 6 presents performance analysis of the relay selection scheme when taking AMC into account. Section 7 concludes the paper.

2 System Model

The considered system model is a single-cell scenario in a cellular system involving relay-assisted D2D communications. As illustrated in Fig. 1, we assume that there are N CUEs, M candidate RUEs, and a pair of DUEs intending to perform D2D communications in the cell, and all of them are controlled by the BS. The M RUEs are candidate relay nodes to aid the two DUEs to form relay-assisted D2D path. Also assume that N CUEs communicate with the BS via N orthogonal channels and the N orthogonal channels are with the same bandwidth. For ease of the expression in the follow sections, we use $\{C_1, C_2, \cdots, C_j, \cdots, C_N\}$ and $\{R_1, R_2, \cdots, R_i, \cdots, R_M\}$ to denote the N CUEs and M RUEs, respectively. Use S and D to denote the source DUE and the destination DUE, respectively. We also assume that there is no idle cellular channel for DUEs, i.e., DUEs must reuse an uplink channel of CUEs to access the system and communicate with each other. If DUEs work on direct D2D mode, the two DUEs reuse only one uplink channel of the CUEs to perform data transmission. If the two DUEs work on relay-assisted D2D mode, the source-to-relay and relay-to-destination transmissions can reuse the same uplink channel of a CUE or two different uplink channels of two CUEs. In the relay-assisted D2D mode, the first-hop and the second-hop (i.e., source-to relay and relay-to-destination) transmissions were performed on two different time slots sequentially. In addition, we further assume that the BS can obtain perfect channel state information (CSI) of all links, including the D2D source-to-relay link, relay-to-destination link, CUE-to-relay link and CUE-to-destination link.

3 Problem Formulation for Relay Selection

In this paper, three criterias, i.e., end-to-end data rate, end-to-end transmission delay, and candidate RUEs' remaining battery time, will be considered in the relay selection procedure of the relay-assisted D2D mode. The relay-assisted D2D mode is used as a supplement the direct D2D mode, which means that only when the direct D2D mode is not available, can the relay-assisted D2D mode be used. The relay selection is a part of the joint scheduling performed at

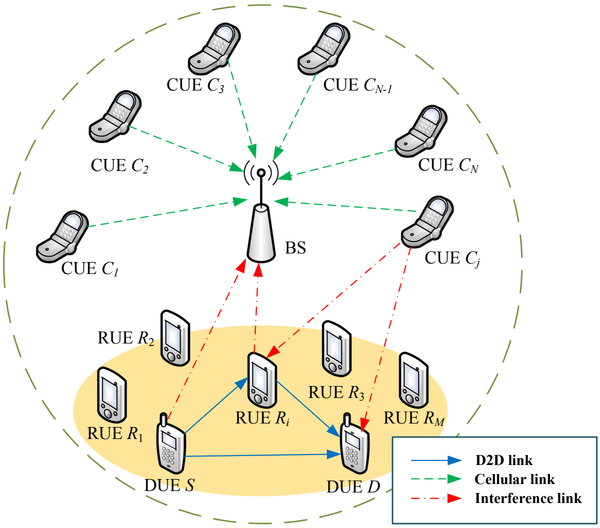

Fig. 1. A single-cell system model for relay-involved D2D communications underlying cellular network, where the uplink channel of CUE C_j is reused by a D2D communication pair in relay-assisted mode (where DUE S and DUE D are the source and destination D2D UEs, respectively, and RUE R_i is the selected relay UE).

the BS side. Once the availability of the relay-assisted D2D mode for two DUEs is being assessed by the BS, it will first try to select an optimal RUE as the relay UE for the two DUEs according to three criterias mentioned above. Hence, the most important thing to do first is to derive the mathematical expressions for the three criterias, based on which the relay selection process can be formulated into a optimization problem, as we have done in our previous work [15]. We have derived the mathematical expressions for the end-to-end data rate and the candidate RUEs' remaining battery time in the previous work. Thus, in this paper, we will put our focus on building an end-to-end transmission delay estimation model while taking the AMC strategy into account. The optimization problem formation for the relay selection process is definitely similar to that in our previous works, so we just make a brief demonstration here. The derivation process of end-to-end transmission delay involving AMC will be presented in Sect. 5. Next we will first provide some knowledge of AMC.

4 Adaptive Modulation and Coding

4.1 Principle of AMC

At physical layer, the channel state is time-varying. To support transmissions of high-speed multimedia services on limited spectrum resources, lots of adaptive technologies have been proposed, link adaptation and AMC. By adjusting transmission parameters according to the available CSI, AMC can improve spectral efficiency and link reliability to maximize data rate.

The schematic diagram for realization of AMC in a wireless communication link is depicted in Fig. 2, in which the AMC selector makes decisions on the mode of modulation and coding according to acquired CSI (e.g., signal to interference and noise ratio, SINR) from the channel estimator, and the decisions are then returned to the transmitter through a feedback channel. The transmitter adjusts modulation and coding scheme (MCS) to adapt changes of the channel. Modulation determines number of data bits that every modulation symbol can transmit, whereas coding provides the function of error correction at the receiver side via pre-adding redundant bits to the data bits before transmission. This is definitely the principle of AMC.

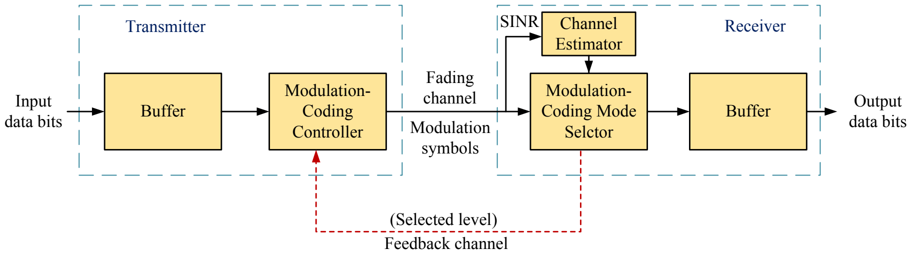

Fig. 2. Schematic diagram of realizing AMC in wireless links

4.2 SINR Boundaries in AMC

As different ranges of SINR corresponds to different MCS levels. In order to select the optimal MCS for a transmission, the SINR boundaries for each MCS level must be decided first. This is also the basis for deriving the end-to-end transmission delay of the relay D2D path in Sect. 5. Let L denote the total number of MCS levels, and we assume that the transmit power is constant. Then divide the entire SINR range into L non-overlapping consecutive intervals, with SINR boundary points denoted as $\{\Gamma_1, \Gamma_2, \cdots, \Gamma_{L+1}\}$. When

$$\gamma \in [\Gamma_l, \Gamma_{l+1}),\ l \in \{1, 2, \cdots, L+1\}, \tag{1}$$

the MCS level l is chosen, where γ is the receive SINR and l is the MCS level index. For the relay-assisted D2D path, γ can be expressed as

$$\gamma_{S,R_i}^{j} = \frac{P_S \left| h_{S,R_i} \right|^2}{P_{C_j} \left| h_{C_j,R_i} \right|^2 + \sigma^2}, \tag{2}$$

and

$$\gamma_{R_i,D}^{k} = \frac{P_{R_i} \left| h_{R_i,D} \right|^2}{P_{C_k} \left| h_{C_k,D} \right|^2 + \sigma^2}, \tag{3}$$

where γ_{S,R_i}^j represents the SINR of S-R_i link (reuse the uplink channel of CUE C_j) and $\gamma_{R_i,D}^k$ represents the SINR of R_i-D link (reuse the uplink channel of CUE C_k). P_S, P_{R_i} and P_{C_j} represent transmit power of the source DUE S, relay UE R_i, and CUE C_j, respectively. $|h_{S,R_i}|^2$, $|h_{C_j,R_i}|^2$, $|h_{R_i,D}|^2$, and $|h_{C_k,D}|^2$ denote the channel gains of $S-R_i$, C_j-R_i, R_i-D, and C_k-D links, respectively. σ^2 is the variance of additive white Gaussian noise (AWGN). Based on the relationship between SINR and packet error rate (PER), the minimum required SINR for the MCS level l can be obtained for a given target PER [16]. And then we can set the boundary Γ_l for the MCS level l equalling to the minimum SINR. With the obtained Γ_l, the SINR boundaries for different MCS levels can be set.

5 End-to-End Transmission Delay Analysis with AMC

In this section, derivation process of end-to-end transmission delay of the relay D2D path will be presented. A queuing model considering AMC will be established to evaluate the end-to-end transmission delay for each D2D path (source-to-relay and relay-to-destination links). To better understand the derivation process of the end-to-end transmission delay, queuing service states transition probability matrix for D2D path will be presented first.

5.1 Queuing Service States Transition Probability Matrix

For a D2D path, the channel is time-varying and different channel states correspond to the different MCS levels. We have assumed that there are L MCS modes, and the L MCS levels available for each D2D link. For each hop of the relay-assisted D2D path, we use c_l to denote the number of data packets that can be transmitted at a time slot (we call it queuing service state) and let $C = \{c_1, c_2, \cdots, c_L\}$ denote the set of queuing service states. Obviously, queuing service state reflects the channel states and is determined by the MCS adopted. In such a case, the set of queuing service state can be described by a finite state Markov chain (FSMC) model. Use $p_{l,m}$ to denote the queuing service state transition probability from c_l to c_m, $(l, m) \in \{1, 2, \cdots, L\}$. It is also assumed that the state transitions only happen between adjacent states, i.e.,

$$p_{l,m} = 0,\ \forall\, |l-m| > 1,\ (l,m) \in \{1, 2, \cdots, L\} \tag{4}$$

Then the adjacent-state transition probability can be determined by [17]

$$p_{l,l+1} = \frac{\chi(\Gamma_{l+1})\Delta T}{\pi_l}, l = 1, \cdots, L-1, \tag{5}$$

and

$$p_{l,l-1} = \frac{\chi(\Gamma_l)\Delta T}{\pi_l}, l = 2, \cdots, L, \tag{6}$$

where π_l is the steady-state probability of state c_l, and ΔT is the duration of a time slot which is set as 1 ms. $\chi(\Gamma_l)$ represents the average number of times per unit interval that a fading signal crosses a given signal level Γ_l. $\chi(\Gamma_l)$ and π_l can be acquired referring the method in [17]. Jointly combining (4), (5), and (6) the state transition probability matrix can be obtained, which will be used in following derivation.

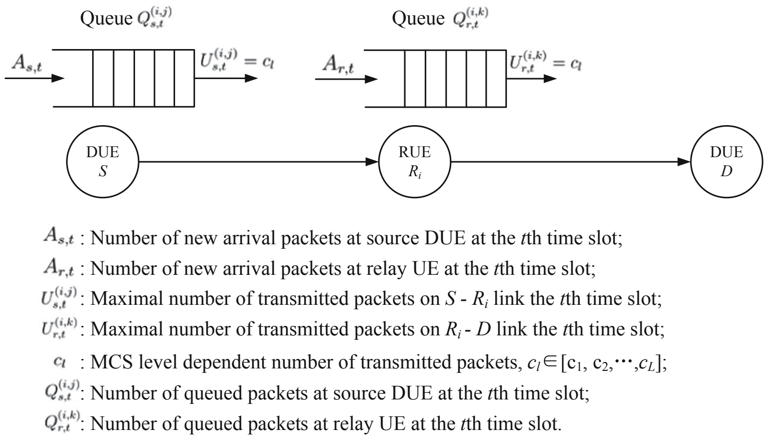

Fig. 3. End-to-end queuing model involving AMC for relay-assisted D2D path, where each UE (except for destination DUE) along the route maintains a fixed-size buffer to store arrived packets.

5.2 A Queuing Model

A queuing model for end-to-end delay estimation of a relay-assisted D2D path combining AMC is illustrated in Fig. 3, where i ($i \in \{1, 2, \cdots, M\}$) denotes the index of RUE, j ($j \in \{1, 2, \cdots, N\}$) denotes the index of CUE whose uplink channel is reused by S-R_i link, and k ($k \in \{1, 2, \cdots, N\}$) denotes the index of CUE whose uplink channel is reused by R_i-D link. To better depict the model, the time axis is evenly divided into time slots, each of which is with a duration of ΔT. When there are new data packets arriving to the source DUE in time slot t, use $A_{s,t}$ to represent the number of data packets arrived, and assume that the packet arrival process is stationary and follows Poisson distribution, i.e.,

$$\mathbb{P}(A_{s,t} = n) = \frac{(\lambda_s \Delta T)^n}{n!} \exp(-\lambda_s \Delta T),\ n \in \{0, 1, 2, \cdots\}, \tag{7}$$

where $\lambda_s \Delta T$ indicates the average number of packets that arrive at the source DUE in a time slot with an arrival rate of λ_s, i.e., the mean of $A_{s,t}$ is $\lambda_S \Delta T$. The arrived packets are stored in a buffer of the source DUE. Assume that the buffer size is K, i.e., the source DUE can store K data packets at most. $Q_{s,t}^{(i,j)}$ denotes the number of packet kept in the source DUE at the end of the tth time slot, and $U_{s,t}^{(i,j)}$ denotes the maximal number of packets that can be transmitted on S-R_i

link in the tth time slot. Obviously, $U_{s,t}^{(i,j)}$ is equal to c_l (number of transmitted data packets determined by AMC at the tth time slot), thus the queuing state transition relationship on S-R_i link can be expressed as

$$Q_{s,t}^{(i,j)} = \min\{K, \max\{0, Q_{s,t-1}^{(i,j)} - U_{s,t}^{(i,j)}\} + A_{s,t}\}, \tag{8}$$

where $Q_{s,t-1}^{(i,j)}$ denotes the number of packets kept in the source DUE at the end of the $(t-1)$th time slot. Then as the data packets arrive at the relay UE, we assume the number of arrival packets is $A_{r,t}$. Obviously, the value of $A_{r,t}$ is correlated with $Q_{s,t-1}^{(i,j)}$ and $U_{s,t}^{(i,j)}$. If $Q_{s,t-1}^{(i,j)} \geq U_{s,t}^{(i,j)} \geq 0$, $A_{r,t} = U_{s,t}^{(i,j)}$; if $U_{s,t}^{(i,j)} \geq Q_{s,t-1}^{(i,j)} \geq 0$, $A_{r,t} = Q_{s,t-1}^{(i,j)}$; otherwise $(U_{s,t}^{(i,j)} = 0)$, $A_{r,t} = 0$.

At the relay UE, buffer size is also set as K, i.e., at most K packets can be stored at a relay UE. In the tth time slot, the number of packets queued in the relay UE's buffer is denoted as $Q_{r,t}^{(i,k)}$ and the maximal number of packets that can be transmitted on the $R_i - D$ link is denoted as $U_{r,t}^{(i,k)}$. Accordingly, the queuing state transition of $R_i - D$ link can be expressed as

$$Q_{r,t}^{(i,k)} = \min\{K, \max\{0, Q_{r,t-1}^{(i,k)} - U_{r,t}^{(i,k)}\} + A_{r,t}\} \tag{9}$$

According to (8), $Q_{s,t}^{(i,j)}$ is closely related to $Q_{s,t-1}^{(i,j)}$, $U_{s,t}^{(i,j)}$, and $A_{s,t}$. As $A_{s,t}$ follows Poisson distribution and is independent of $Q_{s,t-1}^{(i,j)}$ and $U_{s,t}^{(i,j)}$ according to (7), it can be isolated from state $\{Q_{s,t-1}^{(i,j)}, U_{s,t}^{(i,j)}\}$, where $Q_{s,t-1}^{(i,j)}$ and $U_{s,t}^{(i,j)}$ are closely related. To analyze the system behavior, we use a two-dimension state $\{Q_{s,t-1}^{(i,j)}, U_{s,t}^{(i,j)}\}$ to depict both queuing and servicing states. Generally, the queuing and servicing states transition can be described by a FSMC model, i.e., $Q_{s,t}^{(i,j)}$ is only determined by its former state and $U_{s,t}^{(i,j)}$ (or c_l) is determined by its adjacent-state which has been stated in the previous part.

The queuing and AMC behaviors on $S - R_i$ link can be described by a varying-rate queuing system. To do this, the joint queuing and service state transition probability matix should be first formed. The transition probability from states $(Q_{s,t-1}^{(i,j)} = \varphi_s, U_{s,t}^{(i,j)} = c)$ to state $(Q_{s,t}^{(i,j)} = \theta_s, U_{s,t+1}^{(i,j)} = d)$ can be expressed as

$$p_{(\varphi_s,c),(\theta_s,d)}^{(i,j)} = \mathbb{P}(Q_{s,t}^{(i,j)} = \theta_s, U_{s,t+1}^{(i,j)} = d | Q_{s,t-1}^{(i,j)} = \varphi_s, U_{s,t}^{(i,j)} = c), \tag{10}$$

where $\varphi_s, \theta_s \in [0, 1, 2, \cdots, K]$ and $c, d \in [c_1, c_2, \cdots, c_L]$.

Due to the fact that $U_{s,t+1}^{(i,j)}$ is only dependent on $U_{s,t}^{(i,j)}$, (10) can be further simplified as

$$p_{(\varphi_s,c),(\theta_s,d)}^{(i,j)} = \mathbb{P}(U_{s,t+1}^{(i,j)} = d | U_{s,t}^{(i,j)} = c)\mathbb{P}(Q_{s,t}^{(i,j)} = \theta_s | Q_{s,t-1}^{(i,j)} = \varphi_s, U_{s,t}^{(i,j)} = c), \tag{11}$$

where $\mathbb{P}(U_{s,t+1}^{(i,j)} = d | U_{s,t}^{(i,j)} = c)$ is the element in the channel service state transmission probability matrix which has been obtained in the previous subsection. Thus the key work is to compute $\mathbb{P}(Q_{s,t}^{(i,j)} = \theta_s | Q_{s,t-1}^{(i,j)} = \varphi_s, U_{s,t}^{(i,j)} = c)$ to get the joint state transition probability.

Based on (8), we can obtain

$$\mathbb{P}\left(Q_{s,t}^{(i,j)} = \theta_s | Q_{s,t-1}^{(i,j)} = \varphi_s, U_{s,t}^{(i,j)} = c\right) = \begin{cases} 0, & \text{if } 0 \le \theta_s < K, \theta_s < \max\{0, \varphi_s - c\} \\ \mathbb{P}\left(A_{s,t} = \theta_s - \max\{0, \varphi_s - c\}\right), & \text{if } 0 \le \theta_s < K, \theta_s \ge \max\{0, \varphi_s - c\} \\ 1 - \sum_{\theta_s=0}^{K-1} \mathbb{P}\left(A_{s,t} = \theta_s - \max\{0, \varphi_s - c\}\right), & \text{if } \theta_s = K \end{cases} \tag{12}$$

and then the transition probability from state $(Q_{s,t-1}^{(i,j)} = \varphi_s, U_{s,t}^{(i,j)} = c)$ to state $(Q_{s,t}^{(i,j)} = \theta_s, U_{s,t+1}^{(i,j)} = d)$ can be obtained.

As the queuing process can be modeled as a FSMC, the queuing state will be steady after a sufficiently long time, under which each queuing state $Q_{s,t}^{(i,j)}$ corresponds to a stationary probability. Let $\boldsymbol{\Omega}_s^{(i,j)}$ denote the stationary probability vector for the queuing process on S-R_i link. It can be obtained by

$$\begin{cases} \boldsymbol{\Omega}_s^{(i,j)} = \boldsymbol{\Omega}_s^{(i,j)} \boldsymbol{P}_s^{(i,j)}, \\ \sum_{c=c_1}^{c_L} \sum_{\theta_s=0}^{K} \Omega_{s,(\theta_s,c)}^{(i,j)} = 1, \end{cases} \tag{13}$$

where $\boldsymbol{P}_s^{(i,j)}$ is the queuing and servicing joint states transition probability matrix, whose element can be derived by (11). Let $\Omega_{s,(\theta_s,c)}^{(i,j)}$ denote the stationary probability for the queuing state of the source DUE's buffer, i.e., it corresponds to the situation that queue length at the source DUE buffer is θ_s while the channel state is c. $\Omega_{s,(\theta_s,c)}^{(i,j)}$ then can be expressed as

$$\Omega_{s,(\theta_s,c)}^{(i,j)} = \lim_{t\to\infty} \mathbb{P}(Q_{s,t-1}^{(i,j)} = \theta_s, U_{s,t}^{(i,j)} = c) \tag{14}$$

Apparently, $\Omega_{s,(\theta_s,c)}^{(i,j)}$ is an element of $\boldsymbol{\Omega}_s^{(i,j)}$.

Based on the above, we can further get the average packet queue length $\overline{Q_s}^{(i,j)}$, and its mathematical expression is

$$\overline{Q_s}^{(i,j)} = \sum_{c=c_1}^{c_L} \sum_{\theta_s=0}^{K} \left(\theta_s \times \Omega_{s,(\theta_s,c)}^{(i,j)}\right) \tag{15}$$

Similarly, the average packet queue length $\overline{Q_r}^{(i,k)}$ of R_i-D link can be further derived. The derivation process is depicted in Appendix A.

5.3 End-to-End Delay

There are two main factors leading to the transmission delay on S-R_i link and R_i-D link. One is the buffer queues on devices along the transmission route and the other is the packet retransmissions caused by packet losses and packet errors on the links. In this paper, we only consider the finite-length of the buffers at DUE and RUEs as the causes for packet losses. As the length of buffers are finite, the data packets will be dropped when a buffer is full. Use $\nu_s^{(i,j)}$ to denote the average transmission delay for the packet queuing on the S-R_i link. Then according to the Littles law, $\nu_s^{(i,j)}$ can be expressed as

$$\nu_s^{(i,j)} = \frac{\overline{Q_s}^{(i,j)}}{\mathcal{T}_s^{(i,j)}} = \frac{\overline{Q_s}^{(i,j)}}{\mathbb{E}\left[A_{s,t}\right] \times \left(1 - p_s^{(i,j)}\right)}, \tag{16}$$

where $\overline{Q_s}^{(i,j)}$ denotes the average packet queue length of the source DUEs which has been obtained via (15). $\mathbb{E}\left[A_{s,t}\right]$ is the average number of arrived data packets at the tth time slot and equals to $\lambda_S \mathit{\Delta} T$. $p_s^{(i,j)}$ is the packet loss rate, which can be expressed as

$$p_s^{(i,j)} = \lim_{T\to\infty} \frac{\sum\limits_{t=1}^{T} D_{s,t}^{(i,j)}}{\sum\limits_{t=1}^{T} A_{s,t}}, \tag{17}$$

where $A_{s,t}$ represents the number of new arrived data packets and $D_{s,t}^{(i,j)}$ denotes the dropped packets at the tth time slot. $D_{s,t}^{(i,j)}$ can be expressed as

$$D_{s,t}^{(i,j)} = \max\left[0, A_{s,t} - K + \max\left(0, Q_{s,t-1}^{(i,j)} - U_{s,t}^{(i,j)}\right)\right] \tag{18}$$

According to [15], stationary distribution for $A_{s,t}$, $Q_{s,t-1}^{(i,j)}$, and $U_{s,t}^{(i,j)}$ all exist, and here we use A_s, $Q_s^{(i,j)}$, and $U_s^{(i,j)}$ to denote them respectively. Then we have

$$D_s^{(i,j)} = \max\left[0, A_s - K + \max\left(0, Q_s^{(i,j)} - U_s^{(i,j)}\right)\right], \tag{19}$$

where $A_s = n$, $n \in [0, 1, 2, \cdots]$, $Q_s^{(i,j)} = \theta_s$, $\theta_s \in [0, 1, 2, \cdots, K]$, and $U_s^{(i,j)}$ is determined according to the selected MCS level.

Also referring to our previous work [15], packet loss rate can be obtained as

$$p_s^{(i,j)} = \lim_{T\to\infty} \frac{\sum\limits_{t=1}^{T} D_{s,t}^{(i,j)}}{\sum\limits_{t=1}^{T} A_{s,t}} = \frac{\mathbb{E}\left[D_s^{(i,j)}\right]}{\mathbb{E}\left[A_s\right]} = \frac{\mathbb{E}\left[D_s^{(i,j)}\right]}{\lambda_s \mathit{\Delta} T}, \tag{20}$$

where $E\left[D_s^{(i,j)}\right]$ can be obtained as

$$\mathbb{E}\left[D_s^{(i,j)}\right] = \sum_{n=0}^{\infty} \sum_{\theta_s=0}^{K} D_s^{(i,j)} \times \mathbb{P}\left(A_s = n\right) \times \mathbb{P}\left(Q_s^{(i,j)} = \theta_s\right), \tag{21}$$

in which $\mathbb{P}(A_s = n) = \mathbb{P}(A_{s,t} = n)$. As the stationary probability for the queuing states have been obtained above, combining (19)–(21), the transmission delay on S-R_i link can be obtained. Similarly, the transmission delay $\nu_r^{(i,k)}$ on the R_i-D link can be derived, which is depicted in Appendix B.

Accordingly, the end-to-end transmission delay ν of the entire relay-assisted D2D path can be acquired, i.e.,

$$\nu = \nu_s^{(i,j)} + \nu_r^{(i,k)} \tag{22}$$

If BS captures CSI of all links, it selects the optimal relay UE that corresponds to longer operation time, higher end-to-end data rate, and lower end-to-end transmission delay. The format of the objective function combining these three criterias can be found in [15].

6 Performance Evaluation

In this section, we will assess the end-to-end delay performance of the relay selection scheme when taking into account AMC. A single-cell scenario is established in Matlab environment and the cell radius is set as 500 m. All CUEs are randomly distributed in the cell and only one D2D pair is included, where the source DUE randomly locates at least half of the cell radius away from BS, and the destination DUE locates randomly on a circle centering at the source DUE. All RUEs are randomly distributed in the circular area with the source DUE as its center. The number of data bits in a packet is set as 512. The parameters related to ACM is presented in Table 1, and the maximum SINR boundary is ∞ which is not presented in the table. Other major parameters used in the simulation can be found in Table I of our previous work [15].

Table 1. Major parameters related to AMC.

Level l	R_l (bits/sym)	SINR boundary Γ_l
1	0	0
2	2	2.17
3	4	6.82
4	4	16.94
5	6	40.7

Figure 4 shows the delay performance with different average packet arrival rates at source DUE under two relay selection strategies and different channel bandwidths. The delay performances on the relay selection strategies with and without AMC are compared. It is seen that with a fixed channel bandwidth and relay selection strategy, increasing the average packet arrival rate leads to an increase of the transmission delay. Obviously, when other conditions do not

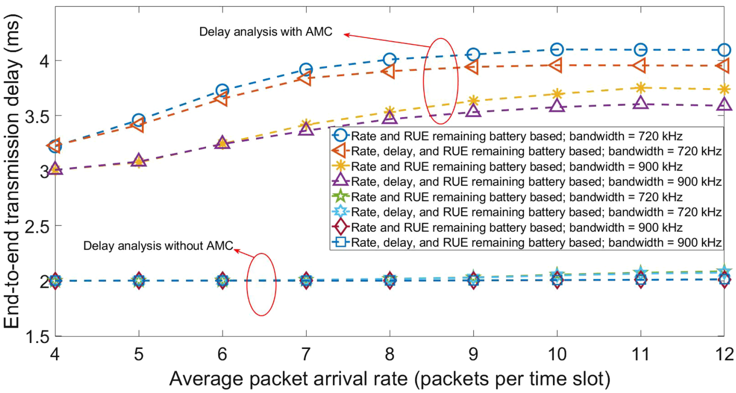

Fig. 4. End-to-end transmission delay versus a varying packet arrival rate at source DUE under different relay selection strategies and channel bandwidths. Channel bandwidths are 720 kHz and 900 kHz, numbers of CUEs and RUEs are 20 and 10, respectively, the distance between source and destination DUEs is 100 m and the buffer size of each UE is 15.

change, increasing arrival rate at DUE S means increasing packet dropping probability at source DUE and the selected RUE due to their finite-length buffers, so the transmission delay on each link will increase. No matter which relay selection strategy is used (either the rate and RUE remaining battery based relay selection strategy or the rate, delay, and RUE remaining battery based relay selection strategy), it is seen that delay will dramatically increase while reducing channel bandwidth, because a smaller bandwidth corresponds to a lower data rate on each link which will decrease the service rate of the queuing system established on each link. The rate and RUE remaining battery based strategy has worse delay performance, while the rate, delay and RUE remaining battery based strategy offers a better delay performance (both in analysis with and without AMC), validating the effectiveness of taking into account the end-to-end delay criteria in relay selection.

In Fig. 4, it is seen that under the same conditions the scheme with AMC corresponds to higher transmission delay than that without AMC. This is reasonable, because the latter always evaluates the performance based on the data rate calculated by Shannon formula, that is, the calculated data rate is always maximal under the current channel condition. The situation with AMC (the data rate is determined by the selected MCS level) shows a more realistic result. In addition, it is seen that with same packet arrival rate and channel bandwidth, the end-to-end delay performance of the rate, delay, and RUE remaining battery based relay selection strategy is better than that of the rate and RUE remaining battery based relay selection strategy.

Figure 5 shows the delay performance with varying distances between DUEs S and D. Increasing separation distance between source and destination DUEs will enlarge the path loss, and result in a decreasing service rate, so the delay

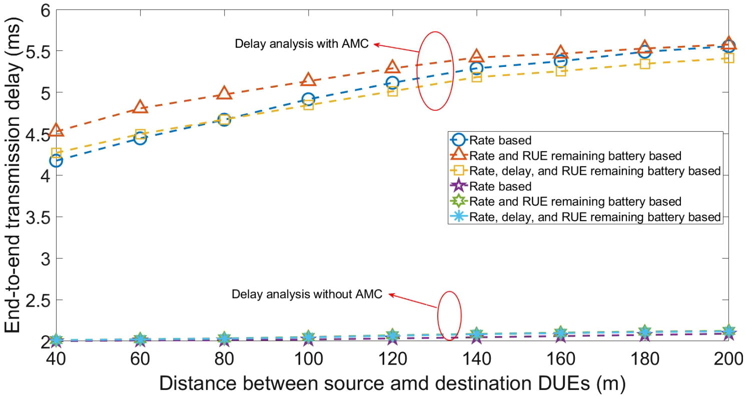

Fig. 5. End-to-end transmission delay versus distance between source and destination DUEs under different relay selection strategies. Channel bandwidth is 720 kHz, the numbers of CUEs and RUEs are 20 and 10, respectively, the average number of packets arrived in each time slot is 10, and the buffer size is 15.

will increase no matter which relay selection strategy is used. It is seen that the strategies with AMC show higher transmission delay than those without AMC due to difference of data rate calculations. In addition, for the strategies without AMC, with same system parameters, the rate based relay selection strategy offers a much better delay performance, compared to other two relay selection strategies. Although the rate based relay selection strategy gives the best delay performance, the fact that RUE remaining battery time is not considered in relay selection may cause that a RUE with short remaining operation time is selected as the relay UE. The rate and RUE remaining battery based strategy has the worst delay performance. While the rate, delay, and RUE remaining battery based strategy offers a delay performance between the other two strategies.

As shown in Fig. 5, for the delay performance with AMC, the rate and RUE remaining battery based strategy still has the worst delay performance. We can notice that the rate based strategy has the best delay performance under certain distance condition, but the rate, delay and RUE remaining battery based strategy will be with the best delay performance when distance is larger than a threshold. The SINR of link is larger while the distance between source and destination nodes is shorter. SINR impacts on the MCS level selection, and higher SINR and corresponding MCS level corresponds to smaller delay, hence the data rate based selection has the best performance while the distance between source and destination DUEs is short. For the relay-assisted D2D mode, although SINR of each link on the relay path may decrease as the distance becomes larger, the entire relay-assisted D2D path may still corresponds to the same MCS level due to the selection cross layer selection criteria.

The delay performance with varying distances between source and destination DUEs under different channel bandwidths is shown in Fig. 6, which only illustrates delay performance with AMC. Only two relay selection strategies are

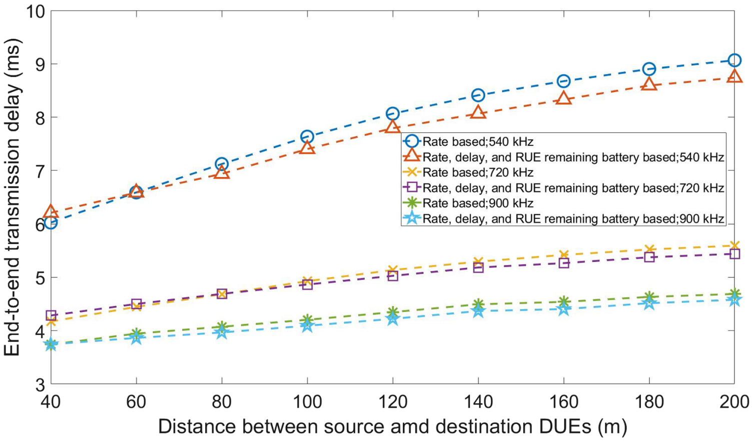

Fig. 6. End-to-end transmission delay versus distance between source and destination DUEs under different relay selection strategies. The numbers of CUEs and RUEs are 20 and 10, respectively, the average number of packets arrived in each time slot is set to 10, and the buffer size of each UEs is 15.

simulated, and the bandwidth' s influence on the delay performance is straightforward.

7 Conclusions

In this paper, we considered the influence of the channels' time-varying property on the relay selection scheme for relay-assisted D2D communication in cellular system. We took into account the delay criteria based on a queuing model involving AMC mechanism. The derivation process for the end-to-end transmission delay of the relay-assisted D2D path was provided. The delay performances were finally evaluated via simulations to validate the effectiveness of the derivation.

A Appendix

We have obtained the queuing states transition relationship of the R_i-D link in (9). We can formulate the transition probability from state $(Q_{r,t-1}^{(i,k)} = \varphi_r, U_{r,t}^{(i,k)} = e)$ to state $(Q_{r,t}^{(i,k)} = \theta_r, U_{r,t+1}^{(i,k)} = f)$ as

$$p_{(\varphi_r,e),(\theta_r,f)}^{(i,k)} = \mathbb{P}(Q_{r,t}^{(i,k)} = \theta_r, U_{r,t+1}^{(i,k)} = f | Q_{r,t-1}^{(i,k)} = \varphi_r, U_{r,t}^{(i,k)} = e), \tag{23}$$

which can also be further expressed as

$$p_{(\varphi_r,e),(\theta_r,f)}^{(i,k)} = \mathbb{P}(U_{r,t+1}^{(i,k)} = f | U_{r,t}^{(i,k)} = e)\mathbb{P}(Q_{r,t}^{(i,k)} = \theta_r | Q_{r,t-1}^{(i,k)} = \varphi_r, U_{r,t}^{(i,k)} = e), \tag{24}$$

where φ_r, $\theta_r \in [0, 1, 2, \cdots, K]$ and e, $f \in [c_1, c_2, \cdots, c_L]$. Similar to (12), we also need acquire the $\mathbb{P}(Q_{r,t}^{(i,k)} = \theta_r | Q_{r,t-1}^{(i,k)} = \varphi_r, U_{r,t}^{(i,k)} = e)$ by

$$\mathbb{P}\left(Q_{r,t}^{(i,k)} = \theta_r | Q_{r,t-1}^{(i,k)} = \varphi_r, U_{r,t}^{(i,k)} = e\right) = \begin{cases} 0, & \text{if } 0 \leq \theta_r < K, \theta_r < \max\{0, \varphi_r - e\}, \\ \mathbb{P}\left(A_{r,t} = \theta_r - \max\{0, \varphi_r - e\}\right), & \text{if } 0 \leq \theta_r < K, \theta_r \geq \max\{0, \varphi_r - e\}, \\ 1 - \sum\limits_{\theta_r=0}^{K-1} \mathbb{P}\left(A_{r,t} = \theta_r - \max\{0, \varphi_r - e\}\right), & \text{if } \theta_r = K. \end{cases} \tag{25}$$

Assume that the number of the arrival packets is ξ. To acquire transition probability, we need to first get the probability of the $A_{r,t}$, i.e., $\mathbb{P}(A_{r,t} = \xi)$. $\mathbb{P}(A_{r,t})$ is related to $U_{s,t}^{(i,j)}$ and $Q_{s,t-1}^{(i,j)}$, which have been discussed in the Subsect. 5.2. We can use $\mathbb{P}\left(Q_{s,t-1}^{(i,j)} = \theta_s, U_{s,t}^{(i,j)} = c\right)$ to replace $\mathbb{P}(A_{r,t})$. Theoretically, we can use stationary probability to replace the transient probability for a specific queue length, i.e., we can use $\lim_{t\to\infty}(Q_{s,t-1}^{(i,j)} = \theta_s, U_{s,t}^{(i,j)} = c)$ replace $\mathrm{P}\left(Q_{s,t-1}^{(i,j)} = \theta_s, U_{s,t}^{(i,j)} = c\right)$. Accordingly, $\mathbb{P}(A_{r,t} = \xi)$ can be expressed as

$$\mathbb{P}\left(A_{r,t} = \xi\right) = \sum_{\theta_s \in [0,1,2,\ldots,K]} \Omega_{s,(\theta_s,c)}^{(i,j)}, \text{ for } (c = \xi, \theta_s > \xi) \text{ or } (c \geq \xi, \theta_s = \xi) \tag{26}$$

Based on the above calculation, the transition probability for queuing state of R_i-D link can be obtained. Similar to S-R_i link, there also exists a stationary probability vector $\boldsymbol{\Omega}_r^{(i,k)}$ for the queuing states of R_i-D link. The calculation of the $\boldsymbol{\Omega}_r^{(i,k)}$ is as

$$\begin{cases} \boldsymbol{\Omega}_r^{(i,k)} = \boldsymbol{\Omega}_r^{(i,k)} \boldsymbol{P}_r^{(i,k)}, \\ \sum\limits_{e=c_1}^{c_L} \sum\limits_{\theta_s=0}^{K} \Omega_{r,(\theta_r,e)}^{(i,k)} = 1, \end{cases} \tag{27}$$

where $\Omega_{r,(\theta_r,\mathrm{e})}^{(i,k)}$ is the element of $\boldsymbol{\Omega}_r^{(i,k)}$, which represents the stationary probability of the state that θ_r packets are queued in the buffer of R_i corresponding to the service state e, i.e.,

$$\Omega_{r,(\theta_r,\mathrm{e})}^{(i,\mathrm{k})} = \lim_{t\to\infty} \mathbb{P}\left(Q_{r,t-1}^{(i,k)} = \theta_r, U_{r,t}^{(i,k)} = e\right). \tag{28}$$

Then the average packet queue length at R_i can be obtained as

$$\bar{Q}_r^{(i,k)} = \sum_{e=c_1}^{c_L} \sum_{\theta_r=0}^{K} \left(\theta_r \times \Omega_{r,(\theta_r,e)}^{(i,k)}\right). \tag{29}$$

B Appendix

Similar to the transmission delay of the S-R_i link, the transmission delay $\nu_r^{(i,k)}$ on the R_i-D link caused by queuing at the buffer of R_i can be expressed as

$$\nu_r^{(i,k)} = \frac{\overline{Q_r}^{(i,k)}}{\mathcal{T}_r^{(i,k)}} = \frac{\bar{Q}_r^{(i,k)}}{\mathbb{E}\left[A_{r,t}\right] \times \left(1 - p_r^{(i,k)}\right)}, \tag{30}$$

where $p_r^{(i,k)}$ denotes the packet loss rate on R_i-D link due to the buffer overflow, $T_r^{(i,k)} = \mathbb{E}\left[A_{\mathrm{r},t}\right] \times \left(1 - p_r^{(i,k)}\right)$ denotes the average throughput of the link, and $\mathbb{E}\left[A_{r,t}\right]$ is the average number of data packets that arrive to R_i in a time slot. $\mathbb{E}\left[A_{r,t}\right]$ can be calculated by

$$\mathbb{E}\left[A_{r,t}\right] = \sum_{\xi=0}^{\min\{K,U_s^{(i,j)}\}} \xi \times \mathbb{P}\left(A_{r,t} = \xi\right), \tag{31}$$

where $\mathbb{P}\left(A_{r,t} = \xi\right)$ is given by (26).

The packet loss rate $p_r^{(i,\mathrm{k})}$ can be calculated as

$$p_r^{(i,k)} = \lim_{T\to\infty} \frac{\sum_{t=1}^{T} D_{r,t}^{(i,k)}}{\sum_{t=1}^{T} A_{r,t}^{(i,k)}} = \frac{\mathbb{E}\left[D_r^{(i,k)}\right]}{\mathbb{E}\left[A_r\right]}, \tag{32}$$

where $D_r^{(i,\mathrm{k})}$ represents the number of dropped packets on the R_i-D link in the tth time slot. According to [15], the stationary distribution $D_r^{(i,\mathrm{k})}$ of $D_{r,t}^{(i,k)}$ can be acquired by

$$\mathbb{E}\left[D_r^{(i,k)}\right] = \sum_{\xi=0}^{\min\{K,U_s^{(i,j)}\}} \sum_{\theta_r=0}^{K} D_r^{(i,k)} \times \mathbb{P}\left(A_r = \xi\right) \times \mathbb{P}\left(Q_r = \theta_r\right), \tag{33}$$

and then $\mathbb{E}\left[D_r^{(i,k)}\right]$ can be further acquired as

$$\mathbb{E}\left[D_r^{(i,k)}\right] = \sum_{\xi=0}^{\min\{K,U_s^{(i,j)}\}} \sum_{\theta_r=0}^{K} \max\left[0, \xi - K + \max\left(0, \theta_r - U_r^{(i,k)}\right)\right] \mathbb{P}(A_r = \xi) \mathbb{P}\left(Q_r^{(i,k)} = \theta_r\right), \tag{34}$$

where $Q_r^{(i,k)} = \theta_r$, $\theta_r \in [0, 1, 2, \ldots, K]$ is the stationary distribution for the queuing states, and $U_r^{(i,k)}$ is determined by the selected MCS level.

By inserting the obtained values of $\mathbb{E}\left[D_r^{(i,k)}\right]$ and $\mathbb{E}[A_r]$ into (32), we can get the transmission delay of R_i-D link.

References

1. Liu, J., Kato, N., Ma, J., Kadowaki, N.: Device-to-device communication in LTE-advanced networks: a survey. IEEE Commun. Surv. Tutor. **17**(4), 1923–1940 (2015)
2. Asadi, A., Wang, Q., Mancuso, V.: A survey on device-to-device communication in cellular networks. IEEE Commun. Surv. Tutor. **16**(4), 1801–1819 (2014)
3. Yu, G., Xu, L., Feng, D., Yin, R., Li, G.Y., Jiang, Y.: Joint mode selection and resource allocation for device-to-device communications. IEEE Trans. Commun. **62**(11), 3814–3824 (2014)
4. Feng, D., Lu, L., Yuan-Wu, Y., Li, G.Y., Feng, G., Li, S.: Device-to-device communications underlaying cellular networks. IEEE Trans. Commun. **61**(8), 3541–3551 (2013)
5. Kim, H., Na, J., Cho, E.: Resource allocation policy to avoid interference between cellular and D2D links/and D2D links in mobile networks. In: The International Conference on Information Networking (ICOIN), pp. 588–591 (2014)
6. Guo, B., Sun, S., Gao, Q.: Power optimization of D2D communications underlying cellular networks in multi-user scenario. In: IEEE International Conference on Communication Systems 2014, pp. 212–216 (2014)
7. Tang, H., Ding, Z.: Mixed mode transmission and resource allocation for D2D communication. IEEE Trans. Wirel. Commun. **15**(1), 162–175 (2016)
8. Hasan, M., Hossain, E., Kim, D.I.: Resource allocation under channel uncertainties for relay-aided device-to-device communication underlaying LTE-A cellular networks. IEEE Trans. Wirel. Commun. **13**(4), 2322–2338 (2014)
9. Hasan, M., Hossain, E.: Distributed resource allocation for relay-aided device-to-device communication: a message passing approach. IEEE Trans. Wirel. Commun. **13**(11), 6326–6341 (2014)
10. Zhou, B., Hu, H., Huang, S., Chen, H.: Intra cluster device-to-device relay algorithm with optimal resource utilization. IEEE Trans. Veh. Technol. **62**(5), 2315–2326 (2013)
11. Nomikos, N., et al.: A survey on buffer-aided relay selection. IEEE Commun. Surv. Tutor. **18**(2), 1073–1097 (2016)
12. Ibrahim, A.S., Sadek, A.K., Su, W., Liug, K.J.R.: Cooperative communications with relay-selection: when to cooperate and whom to cooperate with? IEEE Trans. Wirel. Commun. **7**(7), 2814–2827 (2008)
13. Poulimeneas, D., Charalambous, T., Nomikos, N., Krikidis, I., Vouyioukas, D., Johansson, M.: Delay- and diversity-aware buffer-aided relay selection policies in cooperative networks. In: IEEE Wireless Communications and Networking Conference, pp. 1–6 (2016)
14. Miao, M., Sun, J., Shao, S.: A cross-layer relay selection algorithm for D2D communication system. In: International Conference on Wireless Communication and Sensor Network (WCSN), pp. 448–543 (2014)
15. Ma, R., Chang, Y., Chen, H., Chiu, C.: On relay selection schemes for relay-assisted D2D communications in LTE-a systems. IEEE Trans. Veh. Technol. **66**(9), 8303–8314 (2017)
16. Liu, Q., Zhou, S., Giannakis, G.B.: Queuing with adaptive modulation and coding over wireless links: cross-layer analysis and design. IEEE Trans. Wirel. Commun. **4**(3), 1142–1153 (2005)
17. Zhang, Q., Kassam, S.A.: Finite state Markov model for Rayleigh fading channels. IEEE Trans. Commun. **47**(11), 1688–1692 (1999)